# Why the all-electron full-potential approach is suitable for calculations on fullerenes and nanotubes?

**Yoshiyuki Kawazoe, Kaoru Ohno, Keivan Esfarjani, Yutaka Maruyama, Keiichirou Shiga, and Amir Farajian**

*Institute for Materials Research (IMR), Tohoku University, 2-1-1, Katahira, Aoba-ku, Sendai 980-8577, Japan*

*Already 30 years have passed since the first prediction of $C_{60}$ by Professor Osawa. A family of cage-type fullerenes and carbon nanotubes were experimentally found as the third form of carbon molecules in the 1980s. After this discovery, much research has been conducted experimentally and theoretically on these new materials. The all-electron full-potential approach is important for fully understanding the quantum mechanical behavior of the fullerenes and related molecules. We show some results of band calculations and ab initio molecular dynamics. © 2001 by Elsevier Science Inc.*

*Keywords: mixed-basis, all-electron, fullerene, carbon nanotube*

## INTRODUCTION

Molecules composed of carbon atoms have special physico-chemical properties based on the hybridization of $sp_2$ and $sp_3$ characters. Accordingly, they can have many shapes as stable structures. Two extremes are transparent diamond with complete $sp_3$ hybridization and opaque graphite with complete $sp_2$ hybridization. In between, there are a vast variety of fullerenes, nanotubes, onions, horns, sea urchin, etc., which can be named in various fanciful ways.

The new fullerene-like carbon compounds are basically inexpensive, can be fabricated easily, and have the potential for better functions than other materials. For example, after the era of silicon technology, diamond substrate is now considered to be useful because of the controllability of their ultra-fine size to realize denser integrated circuits. It is known that the number of patents is increasing tremendously concerning the applications of nanotubes and $C_{60}$s as they are expected to be widely useful in industry in the near future.

In this article, we introduce a local density approximation (LDA) formulation using the mixed-basis (the system wavefunction is expanded by a combination of plane waves and atomic orbitals), and demonstrate that this method is efficient for studying carbon-related materials.[1,2] In contrast, highly efficient pseudopotentials are not easy to create for the second row elements. We will also explain briefly the mixed-basis approach and offer several examples.

## METHODS

In the all-electron mixed-basis approach, wavefunctions are expanded by not only plane waves (PWs) but also atomic orbitals (AOs).[1–6] This approach enables one to describe both localized and extended orbitals with a considerably limited number of basis functions. This method has several advantages:

1. Reduction of the number of plane waves
2. Account of core electrons
3. No usage of pseudopotentials
4. Accurate evaluation of matrix elements
5. Absolute value estimation of total energy
6. Minimal memory and CPU time.

Note that the PW-pseudopotential approach requires a large number of plane waves, typically 100,000 even for a single $C_{60}$.[1] Our method can reproduce fairly well the result of Ohtsuki et al.[9] in the fcc $C_{60}$ crystal with much smaller number of PWs[4] of about 5,000. To achieve convergence of electronic states and orthogonalize different electronic levels, we adopt Gram-Schmidt orthogonalization together with a usual steepest descent (SD) algorithm. Moreover, since basis functions are not mutually orthogonal in mixed-basis approach, we start from the modified equation, which guarantees the orthogonality;

Corresponding author: Yoshiyuki Kawazoe, Institute for Materials Research (IMR), Tohoku University, 2-1-1, Katahira, Aoba-ku, Sendai 980-8577, Japan. Tel.:+81-22-215-2050; fax: +81-22-215-2052.

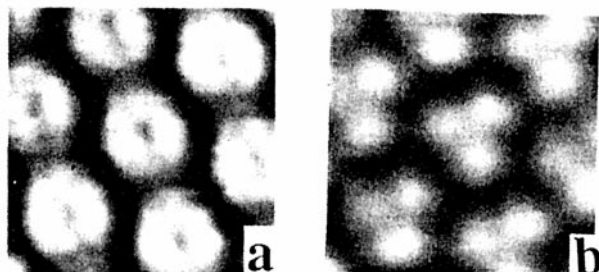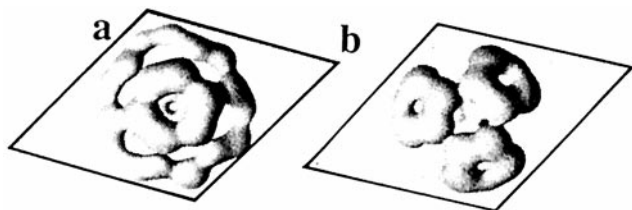*E-mail address*: kawazoe@imr.edu (Y. Kawazoe)

*Figure 1. Spatial PDOS distributions for the first 5 HOMO levels (a) and the first 3 LUMO levels (b) of $C_{60}$ [3], which resemble a doughnut and a three-leaf clover, respectively, observed with the STM by Hashizume et al.[7]*

$$\mu\, S\, \Psi_i = -\,(H - \Psi_i^\dagger\, H\, \Psi_i)\Psi_i, \tag{1}$$

where $\mu$ denotes the friction constant for updating electron wavefunctions $\Psi_i$, $H\ (= <k|\,H\,|l>)$ denotes the Hamiltonian of the electrons, and $E$ denotes the total energy of the system. The distinction of the present equations of the mixed-basis

approach from those of the original pseudopotential approach[1] is the presence of the overlap matrix $S\ (= <k|l>)$ in Equation 1, which is due to the fact that the bases are not mutually orthogonal. Introducing the lower-half triangular matrix $U$, which satisfies $S = UU^\dagger$ by Choleski decomposition[1], and writing $U^\dagger\Psi_i = \Phi_i$ and $H\,' = U^\dagger H U^{\dagger-1}$, we have

$$\mu\, \Phi_i = -\,(H - \Phi_i^\dagger\, H\,'\, \Phi_i)\, \Phi_i. \tag{2}$$

Once we adopt this representation, the main algorithm of updating the wavefunction $\Phi_i$ is the same as the original PW approach. For example, for the case of carbon systems, five AOs ($1s$, $2s$, $2p_x$, $2p_y$, $2p_z$) for each atom and PW (corresponding to the cutoff energy of 7 Ry) are used as a basis set.[3] The core $1s$ AOs are the same as those generated by either the Slater-type orbital (STO) or Herman-Skillman's atomic code, but all the rest of the valence AOs have a truncated tail with cutoff radius of 1.5 Bohr (1 Bohr corresponds 0.52918 Å).

## NUMERICAL SIMULATIONS

### Band Calculations

As the first example of ab initio calculations based on the all-electron mixed basis approach, we show a result of a band calculation of a two-dimensional sheet composed of $C_{60}$. Maruyama et al.[3] carried out a band structure calculation of a two-dimensional array of $C_{60}$. They obtained a good agreement between the resulting HOMO- and LUMO- partial density of states (PDOS) and the scanning tunneling microscopy (STM) images measured by Hashizume et al.[7] for the corresponding $C_{60}$ samples adsorbed on a Cu(111) surface. In the case of an ideal triangular lattice of $C_{60}$ with a lattice constant of 10.2 Å,
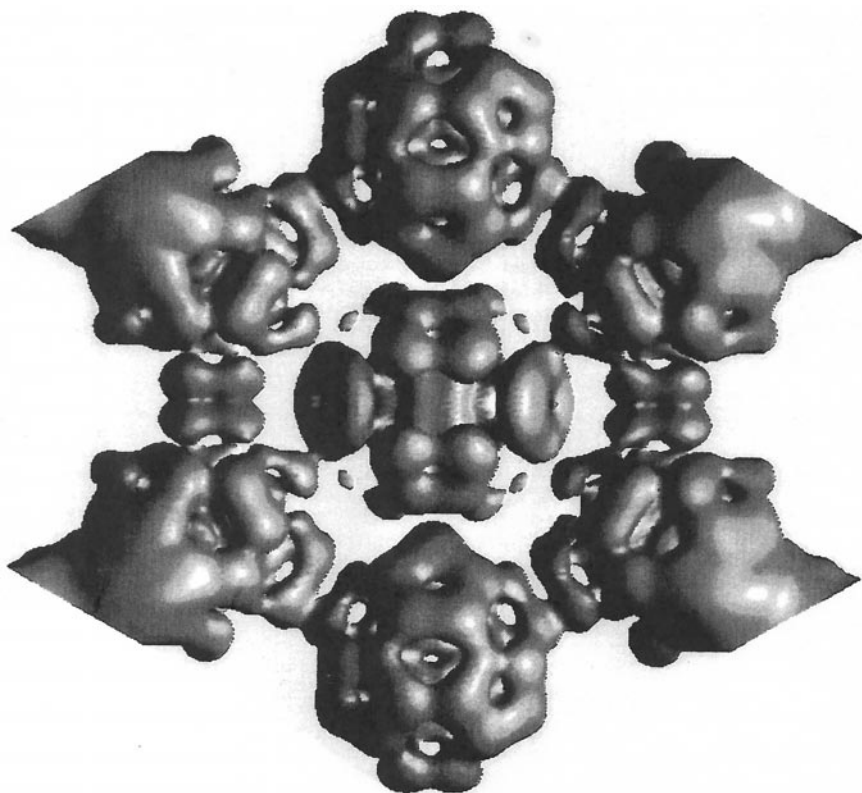


*Figure 2. Spatial PDOS distribution for the first 21 LUMO levels of a $C_{58}+6C_{60}$ heptamer (two-dimensional array) to form a "pretty flower shape" after the irradiation of laser beam. Based on Ohno and Kawazoe.[2])*
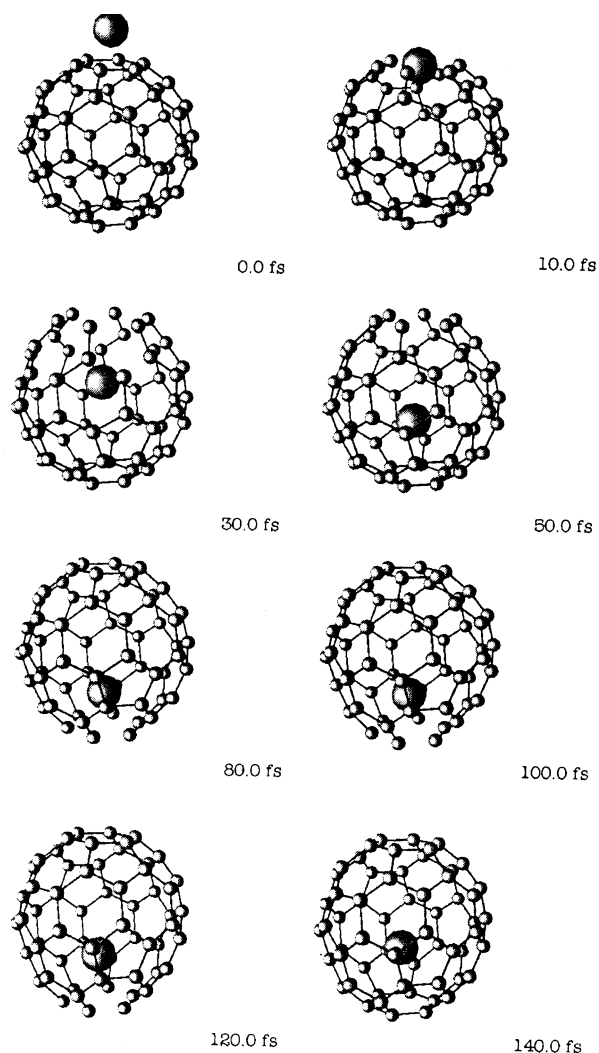
*Figure 3. Snapshots of the insertion process of Xe atom into $C_{60}$ simulated by the ab initio molecular dynamics. In several 10-fm seconds, the atom with 160 eV initial kinetic energy can penetrate through the hexagon hole. Based on Ohtsuki et al.[10]*

the amount of the band gap is calculated to be 1.2 eV. The calculated spatial distributions of PDOS of the first 5 HOMO levels ($h_u$) are highly populated at the double bonds of $C_{60}$, while those of the first 3 LUMO levels ($t_{1u}$) are at the single bonds of $C_{60}$. Thus, the top view of the HOMO-PDOS looks like a doughnut shape and the LUMO-PDOS looks like a three-leaf clover shape as is shown in Figure 1a and Figure 1b, respectively.[3,7] Similarly, Maruyama et al.[3] calculated the band structure of a $C_{60}$–$C_{70}$ mixture alternatively arranged in plane. The HOMO-LUMO gap in this case is estimated to be 1.0 eV because the intrinsic band gap of $C_{70}$ is smaller than that of $C_{60}$ and the shortest interatomic distance between $C_{60}$ and $C_{70}$ is slightly shorter than that in the previous case of pure $C_{60}$.

Ohno and Kawazoe[2] used a larger unit cell to calculate the electronic structure of a similar two-dimensional array of six $C_{60}$ molecules surrounding a center $C_{58}$ molecule, which is made from $C_{60}$ by removing $C_2$ at the topmost double bond. That is, they assumed a hexagonal two-dimensional array of a $C_{58}+6C_{60}$ heptamer. The result may be compared with the STM images of $C_{60}$ samples after laser irradiation.[8] In this calculation, the supercell is divided into $256 \times 256 \times 256$ meshes where one mesh corresponds to 0.116 Å in the xy plane and 0.053 Å in the z direction. The spatial distributions of the PDOS corresponding to the 21 LUMO levels when the isosurface density is relatively small is shown in Figure 2. The figure shows that a small but net density appears over four of the surrounding six $C_{60}$ molecules and extends outward from there. A similar big pattern with six-fold symmetry has been observed experimentally using STM by Kasuya et al.[8] However, it is hard to confirm if this assumed system is identical or not to the one observed experimentally because there is no other evidence except for the similarity of the patterns. In fact, we cannot rule out another possibility such as the adsorption of an external molecule. Therefore, further study is desirable for this subject.

## Molecular Dynamics of Atom Insertion Process to $C_{60}$

Using a supercell approximation and ab initio molecular dynamics based on the all-electron mixed basis approach, Ohno et



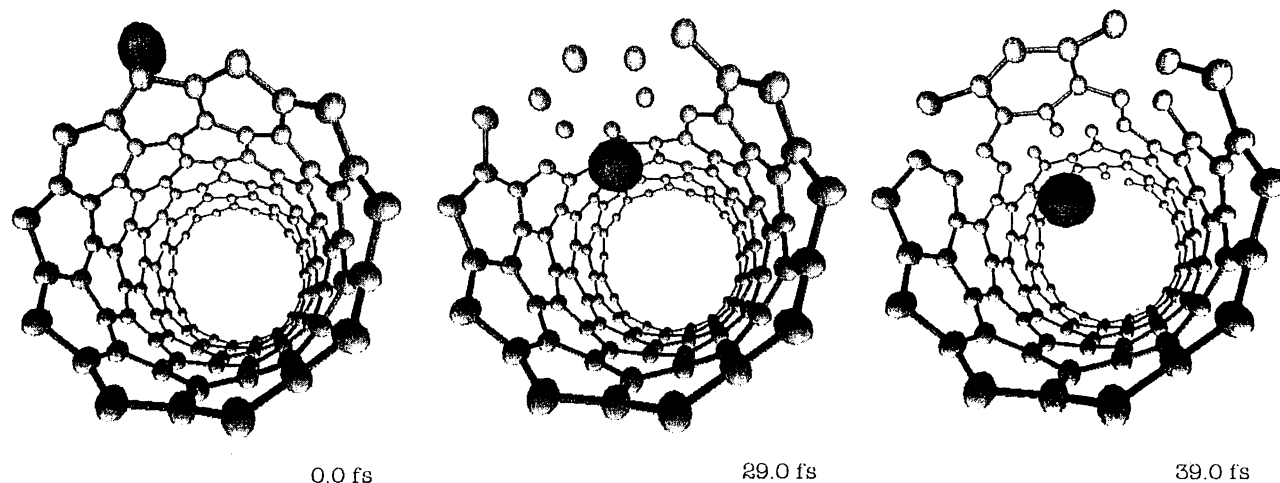*Figure 4. Snapshots of the insertion process of Na atom into carbon nanotube through the hexagon hole simulated by the ab initio molecular dynamics. Based on Farajian et al.[11]*

al.[6] calculated an Li atom insertion into $C_{60}$ through a six-membered ring. In their calculation, the unit-cell is divided into $64 \times 64 \times 64$ meshes, where 2.7 meshes in length correspond to 1 Bohr. For molecular dynamics, they evaluated not only the Hellmann-Feynman force but also the variational force because of the usage of AOs, which are explicitly atomic-position dependent. The basic time step is chosen to be 4 a.u., which corresponds to 0.1 fm second. Later, Ohtsuki et al. calculated Be-insertion,[9] Kr-insertion,[10] and Xe-insertion[10] into $C_{60}$ by using a similar method. Figure 3 shows the snapshots of the Xe-insertion with the kinetic energy of 160 eV. From this figure, one can conceive that Xe atom is finally encapsulated inside the $C_{60}$ cage and forms $Xe@C_{60}$.

## Molecular Dynamics of Atom Insertion Process to Carbon Nanotubes

Using ab initio electronic structure calculation and molecular dynamics, Farajian et al.[11] studied the process of dopant insertion in carbon nanotubes. As a typical example of alkali metals, we consider sodium, for which we obtain the effective potential barrier. This is the barrier seen by an Na atom, which is being inserted into the nanotube through the center of a hexagon in the side wall. Figure 4 shows 3 typical snapshots for this insertion process to understand that the Na atom firstly breaks the hexagon and after the inclusion of it, the broken part is healed. The nanotube is expected to be useful for many purposes. Among them, we have proposed a nanoscale diode with positive and negative ions inserted to the nanotube.[11]

## CONCLUSIONS

Based on the mixed-basis formulation, we have developed an all-electron full-potential computer code to handle core as well as valence electrons accurately with a smaller number of plane waves compared with standard plane-wave-based commercial programs. It has been successfully applied to simulate the quantum mechanical behaviors of fullerenes and carbon nanotubes. At the moment, even if we use dedicated supercomputers, it is impractical to treat systems having several hundreds of atoms for band calculation and 100 fm seconds for ab initio molecular dynamics with approximately 100 atoms.

In the near future, with the fast development of supercomputering power, it will become possible by applying LDA to simulate more complex systems for practical problems including defects and growth processes of these materials and to predict useful properties before experimentation. Another direction of our research is the GW (Green's function – vertex) approximation implemented in the code. So far, we have tested the new GW code to simulate the physical properties of Na clusters. Since the program can predict exactly the values of band gaps, electron affinity, and ionization potential in various materials, it is can be applied to carbon-related materials.

## REFERENCES

1 Ohno, K., Esfarjani, K., and Kawazoe, Y. *Computational Materials Science – From Ab Initio to Monte Carlo Methods.* Springer-Verlag, Berlin, Heidelberg, 1999

2 Ohno, K., and Kawazoe, Y. Theoretical insights into fullerenes adsorbed on surfaces: comparison with STM studies. In: *Advances in Scanning Probe Microscopy*, Springer series on Advances in Materials Research, Vol. 2, Sakurai, T., et al., Eds., Springer-Verlag, Berlin, Heidelberg, 2000, pp. 113–142

3 Maruyama, Y., Ohno, K., and Kawazoe, Y. Electronic structures of $C_{60}$ and $C_{70}$ adsorbed on the Cu(111) surface and intramolecular STM images. *Phys. Rev. B.* 1995, **52**, 2070–2075

4 Gu, B.-L., Maruyama, Y., Yu, J.-Z., Ohno, K., and Kawazoe, Y. Effects of molecular orientation on the electronic structure of fcc $C_{60}$. *Phys. Rev. B.* 1994, **49**, 16202–16206

5 Ohno, K., Maruyama, Y., and Kawazoe, Y. Stability and reactivity of $C_{60}$ studied by all-electron mixed-basis molecular-dynamics simulations at finite temperatures. *Phys. Rev. B.* 1996, **53**, 4078–4082

6 Ohno, K., Maruyama, Y., Esfarjani, K., Kawazoe, Y., Sato, N., Hatakeyama, R., Hirata, T., and Niwano, M. Ab initio molecular dynamics simulations for collision between $C_{60}$ and alkali-metal ions: A possibility of $Li@C_{60}$. *Phys. Rev. Lett.* 1996, **76**, 3590–3593

7 Hashizume, T., Motai, K., Wang, X.D., Shinohara, H., Saito, Y., Maruyama, Y., Ohno, K., Kawazoe, Y., Nishina, Y., Pickering, H.W., Kuk Y., and Sakurai, T. Intramolecular structures of $C_{60}$ molecules adsorbed on the Cu(111)-(1x1) surface. *Phys. Rev. Lett.* 1993, **71**, 2959–2962

8 A. Kasuya, private communication, 2000

9 Ohtsuki, T., Masumoto, K., Ohno, K., Maruyama, Y., Kawazoe, Y., Sueki, K., Kikuchi, K. Insertion of Be atoms in $C_{60}$ fullerene cages: $Be@C_{60}$. *Phys. Rev. Lett.* 1996, **77**, 3522–3524

10 Ohtsuki, T., Ohno, K., Shiga, K., Kawazoe, Y., and Maruyama, Y. Insertion of Xe and Kr atoms into $C_{60}$ and $C_{70}$ fullerenes and the formation of dimers. *Phys. Rev. Lett.* 1998, **81**, 967–970

11 Farajian, A.A., Esfarjani, K., and Kawazoe, Y. Nonlinear coherent transport through doped nanotube junctions. *Phys. Rev. Lett.* 1999, **82**, 5084–5087